JYX JYVÄSKYLÄN YLIOPISTO UNIVERSITY OF JYVÄSKYLÄ

This is a self-archived version of an original article. This version may differ from the original in pagination and typographic details.

Author(s): Koskinen, Pekka; Malola, Sami; Häkkinen, Hannu

Title: Self-passivating reconstructions of graphene edges

Year: 2008

Version: other

Copyright: © 2008 American Physical Society

Rights: In Copyright

Rights url: http://rightsstatements.org/page/InC/1.0/?language=en

Please cite the original version:

Koskinen, P., Malola, S., & Häkkinen, H. (2008). Self-passivating reconstructions of graphene edges. Physical Review Letters, (101), Article 115502. https://doi.org/10.1103/PhysRevLett.101.115502

arXiv:0802.2623v2 [cond-mat.mtrl-sci] 8 Aug 2008

Self-passivating edge reconstructions of graphene

Pekka Koskinen*,[1,†] Sami Malola,[1] and Hannu Häkkinen[1,2]

[1] *Department of Physics, NanoScience Center, 40014 University of Jyväskylä, Finland*
[2] *Department of Chemistry, NanoScience Center, 40014 University of Jyväskylä, Finland*

Planar reconstruction patterns at the zigzag and armchair edges of graphene were investigated with density functional theory. It was unexpectedly found that the zigzag edge is metastable and a planar reconstruction spontaneously takes place at room temperature. The reconstruction changes electronic structure and self-passivates the edge with respect to adsorption of atomic hydrogen from molecular atmosphere.

PACS numbers: 61.46.-w,64.70.Nd,61.48.De,71.15.Mb

Carbon is one of the most prominent elements in nature, vital for biology and life. Although macroscopic carbon has been important since ancient times[1], only modern materials design, utilizing nanotubes[2, 3], fullerenes[4] and single graphene sheets[5], fully attempts to use its flexible chemistry. In applications for nanoscale materials and devices, it is often the atomic and electronic structure of boundaries and surfaces that is responsible for mechanical, electronic and chemical properties.

Since the properties of nanomaterial depend on the precise atomic geometry, its knowledge is crucial for focused preparation of experiments and for worthy theoretical modeling. Only this enables the further development of nanoelectronic components, nanoelectromechanical devices and hydrogen storage materials[3, 6], or the usage of carbon in compound designs[7].

The importance of precise geometry is emphasized in low-dimensional systems. The strong correlations are known to bring up novel phenomena[8], and such should be expected also for the quasi-one-dimensional edges of graphene. The edge chemistry plays even crucial role in the catalyzed growth of carbon nanotubes[9, 10]. Specifically, as two-dimensional carbon has the honeycomb lattice, edge behaviour ultimately boils down to the properties of graphene edges. Hence it is relevant to explore different graphene edge geometries and their chemical properties beyond the standard zigzag and armchair ones.

This relevance is evident from the abundant literature. The electronic properties of graphene as well as carbon nanotube armchair and zigzag edges have been studied extensively[11, 12], often in connection to nanotube growth[9, 13] or the so-called electronic "edge states"[14, 15, 16]. There has been experimental and theoretical work done even on the reconstruction of graphene edges, but they have differed from the basic reconstruction patterns studied in this work. They have involved either edge roughness[15] or more dramatic folding of the edge into a loop[17].

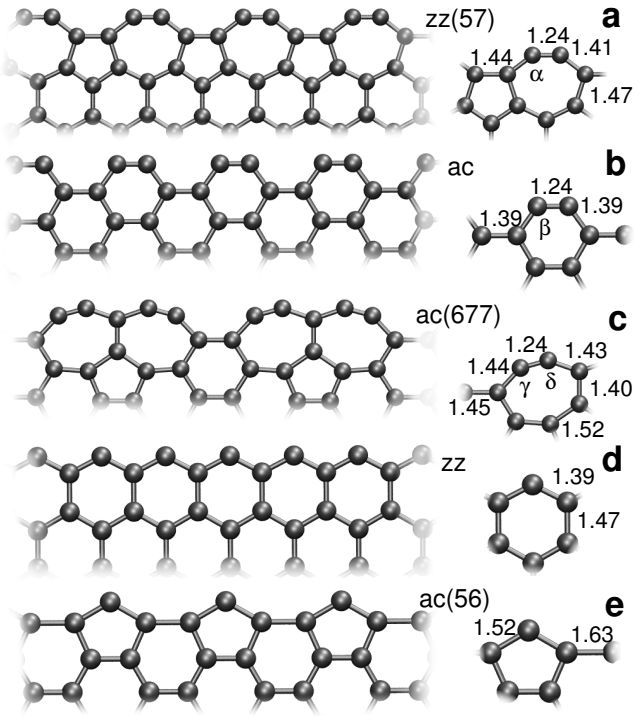

FIG. 1: The geometries of graphene edges. (a) reconstructed zigzag (zz(57)), (b) armchair (ac), (c) reconstructed armchair (ac(677)), (d) zigzag (zz), and (e) pentagonal armchair (ac(56)) edge. The numbers in parentheses denote the number of vertices in edge polygons. Some bond lengths (in Å) and bond angles are shown on the right: the bond angles are $\alpha = 143^\circ$, $\beta = 126^\circ$, $\gamma = 148^\circ$ and $\delta = 147^\circ$. All geometries are strictly in plane.

The edges discussed in this work are shown in figure 1, and were investigated by modeling an infinitely long carbon nanoribbon of a given width (see Methods). Tight-binding method[18] was used to explore number of other edge candidates, but density-functional analysis only for the relevant ones is reported here. The most important edge is zz(57), a reconstruction of zigzag edge

*Author to whom correspondence should be addressed.

where two hexagons transform into a pentagon and a heptagon, like an edge cut through a Haeckelite structure or a line of Stone-Wales defects[19]. The edge ac(677) is a reconstruction of the armchair edge where two separate "armrest" hexagons merge into adjacent heptagons by Stone-Wales mechanism. The pentagonal reconstruction ac(56) of armchair has a slightly different nature, since it requires the diffusion of carbon atoms from distant "armrests" to "seat" positions.

Let us start analysis by looking at edge energy ε_{edge}, which is calculated from the total energy of the graphene ribbon

$$E = -N \cdot \varepsilon_{gr} + L \cdot \varepsilon_{edge},$$

where N is the number of carbon atoms, L the total length of edges (twice the length of simulation cell), and $\varepsilon_{gr} = 7.9$ eV is the cohesion energy of graphene. The edge energies converge rapidly as shown in figure 2 and justify the reference to (semi-infinite) graphene. The energy of armchair edge is 0.33 eV/Å lower than for zigzag edge, in accord with a similar value for nanotubes[10]. However, the principal result is that by edge reconstruction zigzag may lower its energy by 0.35 eV/Å. This implies that the *reconstructed zigzag is the best edge for graphene*. To the best of our knowledge, this is the first report on the metastability of the zigzag edge, which is surprising in view of the abundant literature. Thermal stability of this novel reconstruction was also confirmed with tight-binding simulations[18]. The ac(677) edge has only slightly higher energy than the armchair edge, whereas ac(56) reconstruction has the highest edge energy. We remark that the reconstructions appear to be stable with respect to out-of-plane motion, a situation somewhat different from small-diameter nanotubes[9, 13].

These energetics can be understood by looking at the geometries of figure 1. Previous studies have shown that armchair has low energy due to triple bonds in the "armrests"[12], as realized by comparing their short bonds (1.24 Å) to the bond in acetylene (1.20 Å). Zigzag does not have such triple bonds and ends up with strong and expensive dangling bonds. The reconstructed zz(57) has triple bonds (1.24 Å) but also wider bond angles (143°) which reduces the hybridization energy cost. Triple bonds with wide angles can be observed also in ac(677) edge, but strain in other parts makes the reconstruction unfavoured. The ac(56) edge suffers from dangling bonds like zigzag, and additional high strain energy makes this reconstruction the most expensive one. Regardless, ac(56) edge has relevance during the growth of armchair edges[10].

These observations are supported by hydrogen atom adsorption energies, shown in figure 3. The weak adsorption for armchair (4.36 eV) compared to zigzag (5.36 eV) stems from the triple bonds in the armchair edge. Similarly the weak adsorption for zz(57) (3.82 eV) and ac(677) (3.64 eV) witnesses the weakening of dangling bonds. The adsorption for ac(56) is large because of the strongest dangling bonds. For insight, the adsorption energies in figure 3 are replotted by subtracting hydrogen molecule binding energy $E_{H_2} = 4.58$ eV. The resulting negative number for zz(57) means that the adsorption of hydrogen atom from H_2 molecule is not favored due to cost of H_2 dissociation energy, unless the adsorption process should be complicated[20]. This amounts to the conclusion that *the edge reconstruction chemically passivates zigzag edge*. However, hydrogen adsorption for zigzag+hydrogen edge has yet smaller adsorption energy of 2.14 eV.

The edge energetics are summarized in table I. Note

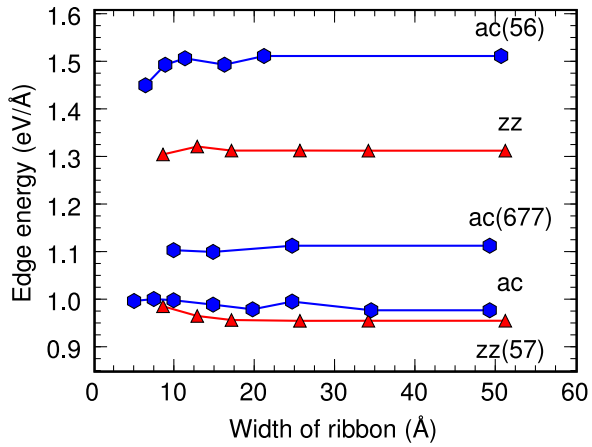

FIG. 2: (color online) The edge energies of carbon nanoribbons. Energies are plotted as a function of the ribbon width for the edges in figure 1.

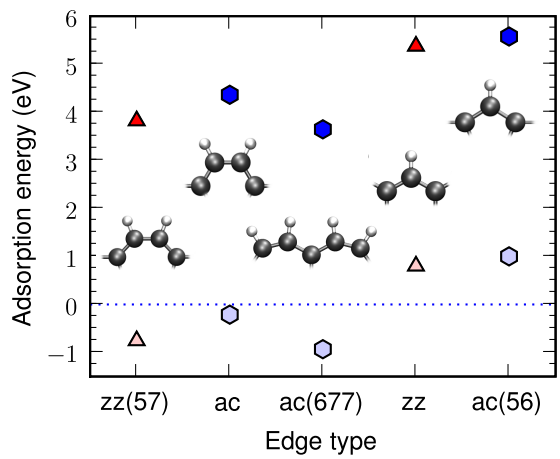

FIG. 3: (color online) Hydrogen adsorption energies. The upper symbols correspond to ε_{ads} with coverage of one hydrogen per edge atom and lower faint symbols are shifted by subtracting the H_2 binding energy; positive $\varepsilon_{ads} - E_{H_2}$ means the hydrogen atom is more strongly bound to the edge than to H_2 molecule.

TABLE I: Summary of the edge and hydrogen adsorption energies. ε^*_{edge} is the energy per edge atom, ε_{ads} the hydrogen adsorption energy with full edge coverage, and $\varepsilon_{edge+ads}$ is the edge energy with hydrogen termination. Note that for ac(56) the edge atom density is $\lambda_{ac(56)} = \lambda_{ac}/2$.

edge	zz(57)	ac	ac(677)	zz	ac(56)
ε_{edge} (eV/Å)	0.96	0.98	1.11	1.31	1.51
ε^*_{edge} (eV/atom)	2.36	2.09	2.30	3.22	6.43
ε_{ads} (eV)	3.82	4.36	3.64	5.36	5.58
$\varepsilon_{edge+ads}$ (eV/Å)	0.34	0.01	0.45	0.06	0.74

that the ordering of edges changes when expressed as energy per edge atom ($\varepsilon^*_{edge} = \varepsilon_{edge}\lambda^{-1}$) due to different edge atom densities $\lambda_{ac} = (2.13\ \text{Å})^{-1}$ and $\lambda_{zz} = (2.46\ \text{Å})^{-1}$. More interesting is to look at edges with hydrogen termination (Klein edge)[16]. For this case the edge energy is $\varepsilon_{edge+ads} = \varepsilon_{edge} - \lambda\cdot(\varepsilon_{ads} - E_{H_2}/2)$, where the reference is to bulk graphene and H_2 molecules. The best edges in this case are normal armchair and zigzag edges because of dangling bonds. On the contrary, the weak dangling bonds and small adsorption energy causes high energies for zz(57) and ac(677) Klein edges.

Let us now concentrate on the thermodynamic and electronic properties of zigzag edges. We would like to clarify an aspect which is ambiguous in the literature: there are two types of electronic zigzag edge states. The so-called "flat band" in figure 4a comes from the bulk π-electrons and is indeed localized at the edge. But the band due to dangling bonds is the one seen in the scanning tunneling microscope (STM) image and is located spatially even beyond the edge (figure 4c). In zz(57) formation of triple bonds is evidenced by the nearly isolated dimers in figure 4d, and the reconstruction removes the dangling bond bands away from the Fermi-level by lifting the degeneracy almost by 5 eV. Hence for zz(57) the STM image shows only the "flat band" states. Because the dangling bond bands shift to elusive energies, also chemical reactivity reduces.

In thermodynamic sense the spontaneous reconstruction of zigzag into zz(57) should be possible, since the activation barrier from the zigzag side is only 0.6 eV, from the reconstructed side 2.4 eV. The G-mode vibration of graphene at 1580 cm^{-1} gives an attempt frequency of $\nu_G \sim 5\cdot 10^{12}$ s^{-1}, and elementary approach yields the rapid rate $\nu_G \cdot \exp(-E_B/k_BT) \approx 4\cdot 10^2$ s^{-1} at room temperature.

The reconstructions predicted in this work are expected to survive on graphite terraces due to the weak interaction (5.6 meV/atom) between the basal planes[21]. Using appropriate sample preparation it should be thus possible to observe the reconstruction. STM images often show irregular and blurred edges, yielding no atomic resolution, but at least for passivated edges armchair predominance is claimed, in agreement with table I[16, 22]. So far samples have been prepared intentionally with hydrogen passivation during heat treatment[22, 23], a situation where reconstruction would not be favored. Alternate routes for observing the reconstruction would be the radial distribution function from neutron diffraction experiments without deuterium atmosphere[23], or detection of triple bond -spawned high-energy modes around 2000 cm^{-1} with Raman spectroscopy.

A further topic is the study of the conductance of various graphene edges, particularly the zz(57) edge found here. The presence of the edge state around the Fermi level makes zz(57) ideal for conductance measurements, in contrast to armchair ribbons where the edge state is absent. This may render zz(57) as an interesting stable model for quasi-one-dimensional carbyne with al-

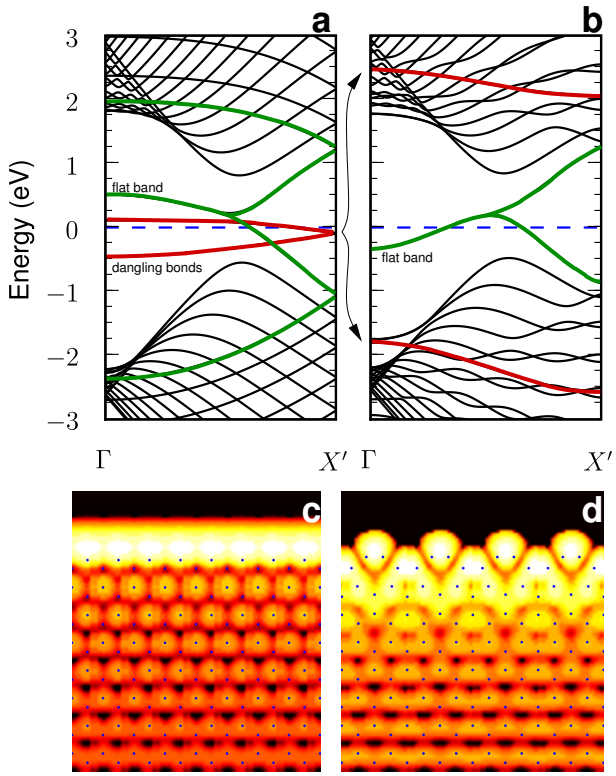

FIG. 4: (color) The electronic structure of zigzag and zz(57) edges. (a) and (b) shows the band structure for 34 Å wide zigzag and zz(57) nanoribbons, respectively, with unit cell width of 4.9 Å. Note that for zigzag this is twice the minimum unit cell and the reciprocal space is thus only half of the normal representation. The dashed line is the Fermi-level. The bands coloured were identified directly by visual inspection of the wave functions. (c) and (d) show the height profiles of simulated scanning tunneling microscope images in constant current mode of the respective edges (height variations > 2 Å), formed by integrating the electron density from occupied bands within 0.1 eV of the Fermi energy. The degeneracies at the gamma-point are 2 and 4 for the dangling bonds and the flat band, respectively.

ternating single and triple bonds. Furthermore, the novel thermodynamically and chemically stable reconstruction could play a role in formation of angular joints in nanoribbons[24], closure of the ends of nanotubes after cutting[25] and any other system where graphene sheets are joined to produce systems with nano-scale morphology.

Methods

We used density-functional theory in conjunction with generalized gradient approximation for the exchange correlation functional[26] and projector augmented waves[27] for the C($2s2p$) electrons, as implemented in GPAW code using real-space grids[28]. Converged energies were obtained with grid spacing of 0.2 Å and 10 **k**-points in the periodic direction. In the perpendicular directions the system is not periodic and the space between the atoms and the wall of the simulation cell was $\geq$ 5.0 Å. The energies were converged to $\sim 10^{-5}$ eV/atom and structures were optimized until forces were less than 0.05 eV/Å. Our calculations agree well with previous relevant experimental as well as theoretical energetic and geometric properties[12, 21]. The activation barrier was calculated with nudged elastic band method[29, 30] by fixing the atoms beyond the first two zigzag-rows with unit cell of length 4.9 Å. The constant current STM of Fig. 4 shows the height profile of electron density isosurface of the occupied states within $\sim$ 0.1 eV energy window below the Fermi-level. The isosurface value corresponds to average density 2 Å above the graphene plane ($3 \cdot 10^{-5}$ electrons/Å^3).

Acknowledgements

We acknowledge support from the Academy of Finland (projects 121701 and 117997) and from the Finnish Cultural Foundation. We thank Matti Manninen for discussions, Michael Walter for technical assistance with GPAW calculations and Karoliina Honkala for reading of the manuscript. The computational resources were provided by the Finnish IT Center for Science (CSC) in Espoo.

† Electronic address: pekka.koskinen@phys.jyu.fi

[1] M. I. Katsnelson, Materials Today **10**, 20 (2007).
[2] S. Ijima, Nature **354**, 56 (1991).
[3] R. H. Baughman, A. A. Zakhidov, and W. A. de Heer, Science **297**, 787 (2002).
[4] H. W. Kroto, J. R. Heath, S. C. O'Brien, R. F. Curl, and R. E. Smalley, Nature **318**, 162 (1985).
[5] J. C. Meyer, A. K. Geim, M. I. Katsnelson, K. S. Novoselov, T. J. Booth, and S. Roth, Nature **446**, 60 (2007).
[6] J. M. Kinaret, T. Nord, and S. Viefers, Appl. Phys. Lett. **82**, 1287 (2003).
[7] S. Stankovich, D. A. Dikin, G. H. B. Dommet, K. M. Kohlhaas, E. J. Zimney, E. A. Stach, R. D. Piner, S. T. Nguyen, and R. S. Ruoff, Nature **442**, 282 (2006).
[8] P. Koskinen, H. Häkkinen, B. Huber, B. von Issendorff, and M. Moseler, Phys. Rev. Lett. **98**, 015701 (2007).
[9] J.-C. Charlier, A. De Vita, X. Blase, and R. Car, Science **275**, 647 (1997).
[10] Y. H. Lee, S. G. Kim, and D. Tomanek, Phys. Rev. Lett. **78**, 2393 (1997).
[11] K. Nakada, M. Fujita, G. Dresselhaus, and M. S. Dresselhaus, Phys. Rev. B **54**, 17954 (1996).
[12] T. Kawai, Y. Miyamoto, O. Sugino, and Y. Koga, Phys. Rev. B **62**, R16349 (2000).
[13] E. Hernandez, P. Ordejon, I. Boustani, A. Rubio, and J. A. Alonso, J. Chem. Phys. **113**, 3814 (2000).
[14] D. Jiang, B. G. Sumpter, and S. Dai, J. Chem. Phys. **126**, 134701 (2007).
[15] D. Gunlycke, D. A. Areshkin, and C. T. White, Appl. Phys. Lett. **90**, 142104 (2007).
[16] Y. Kobayashi, K.-I. Fukui, T. Enoki, and K. Kusakabe, Phys. Rev. B **73**, 125415 (2006).
[17] K. Jian, A. Yan, I. Kulaots, G. P. Crawford, and R. Hurt, Carbon **44**, 2105 (2006).
[18] D. Porezag, T. Frauenheim, T. Köhler, G. Seifert, and R. Kaschner, Phys. Rev. B **51**, 12947 (1995).
[19] A. J. Stone and D. J. Wales, Chem. Phys. Lett. **128**, 501 (1986).
[20] X. Sha and B. Jackson, J. Am. Chem. Soc. **126**, 13094 (2004).
[21] X. Hua, T. Cagin, J. Che, and W. A. Goddard III, Nanotechnology **11**, 85 (2000).
[22] Y. Kobayashi, K.-I. Fukui, T. Enoki, K. Kusakabe, and Y. Kaburagi, Phys. Rev. B **71**, 193406 (2005).
[23] T. Fukunaga, K. Itoh, S. Orimo, M. Aoki, and H. Fujii, J. Alloys Compd. **327**, 224 (2001).
[24] X. Li, X. Wang, L. Zhang, S. Lee, and H. Dai, Science **319**, 1229 (2008).
[25] Y. Gan, J. Kotakoski, A. V. Krasheninnikov, K. Nordlund, and F. Banhart, New J. Phys. **10**, 023022 (2008).
[26] J. P. Perdew, K. Burke, and M. Ernzerhof, Phys. Rev. Lett. **77**, 3865 (1996).
[27] P. E. Blöchl, Phys. Rev. B **50**, 17953 (1994).
[28] *GPAW wiki*, URL `https://wiki.fysik.dtu.dk/gpaw`.
[29] G. Henkelman and H. Jonsson, J. Chem. Phys. **113**, 9978 (2000).
[30] E. Bitzek, P. Koskinen, F. Gähler, M. Moseler, and P. Gumbsh, Phys. Rev. Lett. **97**, 170201 (2006).